Discharge Coefficient of a C-Type Piano Key Side Weir at 30° and 120° Sections of a Curved Channel

Yaser Mehri [a], Jaber Soltani [b*], Mojtaba Saneie [c], Mohammad Rostami [d]

[a] *Post Graduate, Department of Irrigation Engineering, Aburaihan Campus, University of Tehran, Iran.*

[b] *Assistant professor, Department of Irrigation Engineering, Aburaihan Campus, University of Tehran, Iran.*

[c] *Associate Professor, Dept. of River Engineering, Soil Conservation and Watershed Management Research Institute, Iran.*

[d] *Assistant Professor, Dept. of River Engineering, Soil Conservation and Watershed Management Research Institute, Iran.*

Abstract

A piano key side weir (PKSW) is a non-linear weir that discharge exceeds linear weirs by increasing the length in width. PKSW can be used in side weirs with space limitation. As side weirs are extensively used in flood control, water level control in rivers, and water supply channels, it is necessary to use PKSW as side weirs. This research discusses the discharge coefficient of a PKSW by assessing a C-type PKSW at 30° and 120° sections of a channel with a longitudinal curve. Dimensional analysis was used for identifying the parameters effective in the discharge coefficient. The effects of these parameters are examined by analysing the effective parameters. Finally, an empirical relationship has been proposed for determining the discharge coefficient based on the dimensionless parameters for calculating the discharge coefficient with the correlation coefficient of 0.88 and the mean error of 0.091. The influence of the $P/h1$ parameter on the PKSW is more than that of the remaining parameters: With an increase in the value of this parameter, considering decreases in the length of the deviation and a lack of submerged inlet keys, the coefficient of discharge increases.

Keywords: Non-Linear Weir; Piano Key Side Weir (PKSW); Curved Channel; Empirical Equation; Dimensional Analysis.

1. Introduction

The length of weirs should be increased to improve and raise the discharges of side weirs. However, certain problems occur when this method is applied to achieve this goal. One problem is to raise the costs for constructing and designing an outlet side channel with respect to the increasing length of a weir, while another problem pertains to the inapplicability of this method in mountainous areas, meanders, and places with abundant curves due to design and environmental limitations. Therefore, it is necessary to find an appropriate solution for this problem. A side weir is responsible for discharging an additional flow from the main route in urban sewage systems, irrigation and drainage networks, and flood control in a river and controlling water levels [1, 2]. One method to improve the hydraulic performance of side weirs is to increase the discharge capacity of the weirs. Piano Key Side Weirs (PKSWs) are the new types of non-linear weirs that outperform other linear weirs in terms of inlet width, discharge volume, and the height of water collected behind a weir. They combine a labyrinth weir through inlet and outlet keys [3]. PKSWs are generally divided into four categories, as shown by Figure 1.
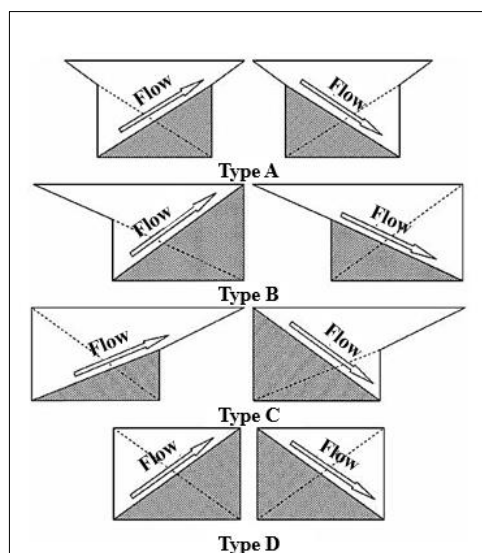

Figure 1. Types of PKSW [4]

Studies have generally focused on rectangular or triangular weirs in a direct channel. Only a handful of studies are conducted on side weirs in curved channels and meanders, while research results are not appropriate for curved channels [5]. Agaccioglu and Yüksel [6] have studied a sharp-crested side weir in a curve channel and presented an empirical relation for rectangular sharp-crested side weirs in a curved channel. Coşar and Agaccioglu [7] have used a triangular side-weir in a curved channel and studied the hydraulic features of the weirs in a curve. Agaccioglu et al. [8] have studied and analyzed the impact of a side weir at the 30° section of a curve on a sediment bed scour. Kaya et al. [9] have used a semi-elliptical weir in a direct channel as a side weir. Emiroglu and Kaya [10] have evaluated the flow rate coefficient of a trapezoidal labyrinth side weir in a direct main channel with varied dimensions and cross-sections. Vatankhah [11] has conducted an analytical and mathematical analysis on the water surface profile as well as on a side weir in a channel with trapezoidal cross-sections. Vatankhah [12] also carried out an analytical and mathematical analysis on the water surface profile and the discharge capacity of a sharp-crested rectangular side weir in a channel with an elliptical cross-section. Azimi and Shabanlou [13] numerically studied the flow pattern in a triangular cross-section channel for a rectangular side weir.

Aydin and Emiroglu [14] have evaluated the capability of numerical models in predicting flow conditions through the numerical simulation of a labyrinth weir in a direct channel. Tiwari and Sharma [15] have studied the turbulent kinetic energy in the upstream of the piano key weir. Ghasem Zadeh et al. [16] used the FLOW 3D software to simulate the flow through a paino key side weir in straight channel. The flow 3D software was used for numerical analysis. Firstly completed a physical model study to evaluate discharge vs. head relationships of PK weirs. In this study, was compared the Stage discharge relation of the experimental model and 3D flow numerical simulations. Results show that the CFD model was able to simulation the stage discharge relation better than of the physical model. Hu, Han, et al. [17] Numerical study of characteristics and discharge capacity of piano key weirs. A comprehensive numerical investigation was performed to better understand the flow patterns of Piano Key weirs (PKW) for different upstream heads, based on the volume-of-fluid model. The results of numerical simulation indicate that, the efficiency of side crests are limited by following factors: the change of side crest flow direction caused by the effect of the longitudinal flow velocity along the inlet keys, submerged flow regime in outlet keys, interference between nappes, and the head loss along the inlet keys, under the conditions of high upstream head, which eventually leads to the decrease in discharge efficiency with an increase in the upstream head.

Al-Shukur, et al. [18] Experimental study of the hydraulic performance of piano key weir. In this study, laboratory experiments were performed to evaluate the effects of the weir geometry of a Piano Key Weir (PKW) type B on the discharge coefficient under free flow conditions. Experimental results showed that the most influential parameters for the tested PKW models are the relative length L/W and height difference between up and downstream Pi/Po, both increasing the discharge capacity by 42%. Also the energy dispassion was estimated from the parameter B/P by considering the effect of slope (B the base and P the height) on distance of hydraulic jump formation. Then, the PKW angle which makes it an energy dissipater itself has been selected. Experimental data were used to develop empirical formula based on dimensional analysis technique and the statistical software SPSS. This formula, having a coefficient of determination of (R^2=0.984), is used to find the discharge coefficient during free flow condition. Mehboudi, et al. [19] Experimental study of discharge coefficient for trapezoidal piano key weirs (TPKW). In this experimental study, geometrical parameters of TPKW models were varied under different flow conditions and effects on discharge coefficient (Cd) were investigated. The Cd values were found to be mostly influenced by L/W whereas Wi/Wo had the least effect. Results also showed that TPKW has higher discharge efficiency in comparison with RPKW. This was

believed to be related to formation of an "interference wedge" over the TPKW. Finally, quantitative values for distinguishing three flow regimes (i.e. nappe, transition and submergence) as well as criteria for design of TPKW are proposed.

The present research aims to evaluate the discharge coefficient of a PKSW at 30° and 120° sections of a curve, thereby proposing an empirical equation to determine the discharge coefficient of the weirs by comparing the results and selecting the appropriate weir.

2. Materials and Methods

2.1. Side Weir Principles

Equation 1 shows the differential equation governing the spatial variable flow with flow rate reduction:

$$\frac{dy}{ds} = \frac{S_0 - S_f - (\frac{Q}{gA^2})(\frac{dQ}{dx})}{1 - (\frac{Q^2 b}{gA^3})} \tag{1}$$

Where s is the transverse axis of the side weir gap, S_o is the main channel gradient, S_f is the energy gradient, Q is the main channel flow rate, $dQ/ds = q$ is the flow rate of the width unit of the side weir, and y is the flow level changes. DeMarchi [20], made some assumptions which solved the flow over side weir analytically. Ignoring the friction and assuming constant specific energy along lateral weir are the main assumptions made by him. Based on these assumptions $dE/dX = q$, he presented the equation by solving analytically. The flow rate in the width unit of the side weirs can be shown in Equation 2.

$$q = \frac{-dQ}{ds} = C_d \frac{2}{3} \sqrt{2g} (h - p)^{\frac{3}{2}} \tag{2}$$

Where dQ/ds equals the changes of flow rate in the width unit of side weirs, Q is the total flow rate in the main channel, c_d is the flow rate coefficient (De-Marchi coefficient), g is the acceleration of gravity, h is the water height on the weir, and P is the weir height. Table 1 shows some of the equations for calculating the weir discharge coefficient. Equation 3 shows the parameters effective in the discharge coefficient of the PKSW.

$$C_d = f(b, h_1, V_1, L, g, S_0, \Psi, \nu, \sigma, r_C, \rho, P, n, p_d, l, w_i, w_o, B, S_{in}, S_{out}, \alpha) \tag{3}$$

Where C_d is the weir discharge coefficient, b is the channel width, h_1 is the depth of flow on the upstream edge of the weir, V_1 is the flow velocity on the first edge of the weir, L is the weir gap width, g is the acceleration of gravity, S_0 is the channel gradient, ψ is the angle of the flow deviation, ν is the kinematic viscosity, σ is the surface tension, r_c is the channel radius from the central axis of the channel, ρ is the flow density, P is the total height of the weir, n is the Manning coefficient of the weir, P_d is the weir base, l is the effective length of the weir, w_i is the width of the inlet key, w_0 is the width of the outlet key, B is the length of the weir along the flow, S_{in} is the gradient of the inlet key, S_{out} is the gradient of the outlet key, α is the angle of the PKSW. Borghei et al. [21] have shown that the effects of Manning coefficient and gradient were low; they were negligible in the discharge coefficient of side weirs and could be overlooked. As the depth of the flow on the weir was considered to be over 30 mm, surface tension could also be overlooked.

In this research, S_{in} and S_{out} were considered identical for all the weirs. Studies show that they have no impact on the discharge coefficient of the weir. $w_i/w_0 = 1$ was considered in the weir design. The weir effective length is a function of the weir gap width, as 5L=l for all models. Therefore, Table 1 shows the equations presented by researchers on the discharge coefficient.

$$C_d = f(b, h_1, V_1, L, g, r_C, \rho, P, p_d, B, \alpha) \tag{4}$$

Table 1. The equations for calculating discharge coefficient

No	Discharge Coefficient	References
1	$$C_d = 0.866\left(\frac{1-F_1^2}{2+F_1^2}\right)^{0.5}$$	Subramanya and Awasthy [22]
2	$$C_d = 0.432\left(\frac{2-F_1^2}{1+2F_1^2}\right)^{0.5}$$	Nandesamoorthy and Thomson [23]
3	$$C_d = 0.485\left(2+\frac{F_1^2}{2}+3F_1^2\right)^{0.5}$$	Hager [24]
4	$$C_d = 0.81 - 0.6F_1$$	Ranga Raju et al. [25]
5	$$C_d = 0.33 - 18F_1 + 0.49\frac{P}{h_1}$$	Singh et al.[26]
6	$$C_d = 0.7 - 0.48F_1 - 0.3\frac{P}{h_1} + 0.06\frac{L}{b}$$	Borghei et al. [21]
7	$$C_d = 0.96 - 0.0612F_1 + 0.5135F_1^2$$	Coşar and Agaccioglu [7]
8	$$C_d = 0.432 + 0.016\left[\begin{array}{l}1.3(\frac{P}{h_1})^{4.07}+1.07(\frac{L}{b})^{1.81}-\\0.65.95(\frac{L}{R_C})^{2.65}+\\0.007\left(0.72+\sin\frac{a}{4}\right)^{13.15}+1.09F_1^{0.955}\end{array}\right]^{4.38}$$	Agaccioglu et al [5]

2.2. Dimensional Analysis

In principle, dimensional analysis refers to the categorization of effective variables, reduction of the number of variables effective in terms of physical phenomena, and their conversion into fewer dimensionless groups of the same variables in a physical phenomenon. All physical quantities can be expressed in terms of several main dimensions.

2.2.1. Buckingham Theorem

This theorem expresses that n quantities of $x_1, x_2, \ldots$ and x_n effective in a physical phenomenon can be shown as (n-m) dimension group of that quantity. M is number of the main dimensions required for the dimensional display of quantities. Dimensionless groups are shown by Π. Therefore, the following function:

$$f_1(x_1, x_2, x_3, \ldots, x_n) \tag{5}$$

Can be expressed by Equation 6.

$$f_1\left(\prod_1, \prod_2, \prod_3, \ldots, \prod_{n-m}\right) \tag{6}$$

Each Π has m repeated quantities encompassing a total m dimensional dimensions. In hydraulics, m generally Equals 3. In general, the forces that may apply on a fluid particle to conduct a dimensional analysis should be selected among the repeated effective parameters. The method of Buckingham was used to calculate dimensionless parameters. For this purpose ρ, g, and h_1 parameters were selected as the effective repeated parameters. Hence, 10 out of 13 parameters were selected as independent parameters in Equation 4. Using the dimensional analysis, the following dimensionless parameters were obtained:

$$\prod_3 = \frac{L}{h_1}, \ \prod_4 = \frac{r_c}{h_1}, \ \prod_5 = \frac{p}{h_1}, \ \prod_6 = \frac{p_d}{h_1}, \ \prod_7 = \frac{B}{h_1}, \ \prod_8 = C_d, \ \prod_9 = \psi \tag{7}$$

After simplification of the above relation, we will have:

$$\frac{\prod_3}{\prod_1} = \frac{L}{b}, \ \frac{\prod_3}{\prod_4} = \frac{L}{r_c}, \ \frac{\prod_6}{\prod_7} = \frac{p_d}{B} \tag{8}$$

Finally, the parameters effective in discharge coefficient can be shown by Equation 5 with respect to the above

relations:

$$C_d = f(\frac{L}{b}, F_1, \frac{L}{r_c}, \frac{p}{h_1}, \frac{p_d}{B}, \psi, \alpha) \tag{9}$$

With a view to the earlier studies, ψ as per Equation 10, is a Froude number and it can be removed from Equation 9.

$$Sin\,\psi = \sqrt{1 - \left(\frac{3F_1^2}{F_1^2 + 2}\right)} \tag{10}$$

Therefore, Equation 10 can be shown as Equation 11:

$$C_d = f(\frac{L}{b}, F_1, \frac{L}{r_c}, \frac{p}{h_1}, \frac{p_d}{B}, \alpha) \tag{11}$$

2.3. Experimental Setup

All experiments were conducted in a closed-loop rectangular Plexiglass flume with curve 180°. This setup is located in Soil Conservation and Watershed Management Research Institute (SCWMRI), Tehran, Iran. Cross section area of the flume is 500×500 mm^2 and the internal radius of the curve is 2 meters. The bottom slop of the canal is 0.001. To uniform the inlet flow, a baffle was used at the entrance of the main canal such that the minimum head loss is observed in the main channel. A C-Type Piano Key Side Weir (PKSW), also known as a lateral weir, is a free-overflow weir set into the side of a channel which allows a part of the liquid to spill over the side when the surface of the flow in the channel rises above the weir crest. The research tests were conducted at 30° and 120° sections of a curved channel. Table 2 shows the channel variables. The tests were designed and conducted on a C-Type PKSW side weir in "based" and "base-free" modes. Table 3 shows the weirs specifications. After flowing into the main channel, water discharges from the reservoir at the angles of 30° and 120° considered in the PKSW and the flow passing the weir is measured by a calibrated rectangular weir in a secondary drainage channel. There was also a triangular weir for measuring the flow rate passing the flume downstream, as the water supply system operated as a closed circuit. In each test, water depth was measured in a mesh consisting of water depth at the edge of the main wall, in the center of the main channel, side channel input and also the water height in the weir a digital depth gauge. A point level meter was used to measure water level profile. Figure 2 shows a C-type PKSW, channel schematic, and weir location.
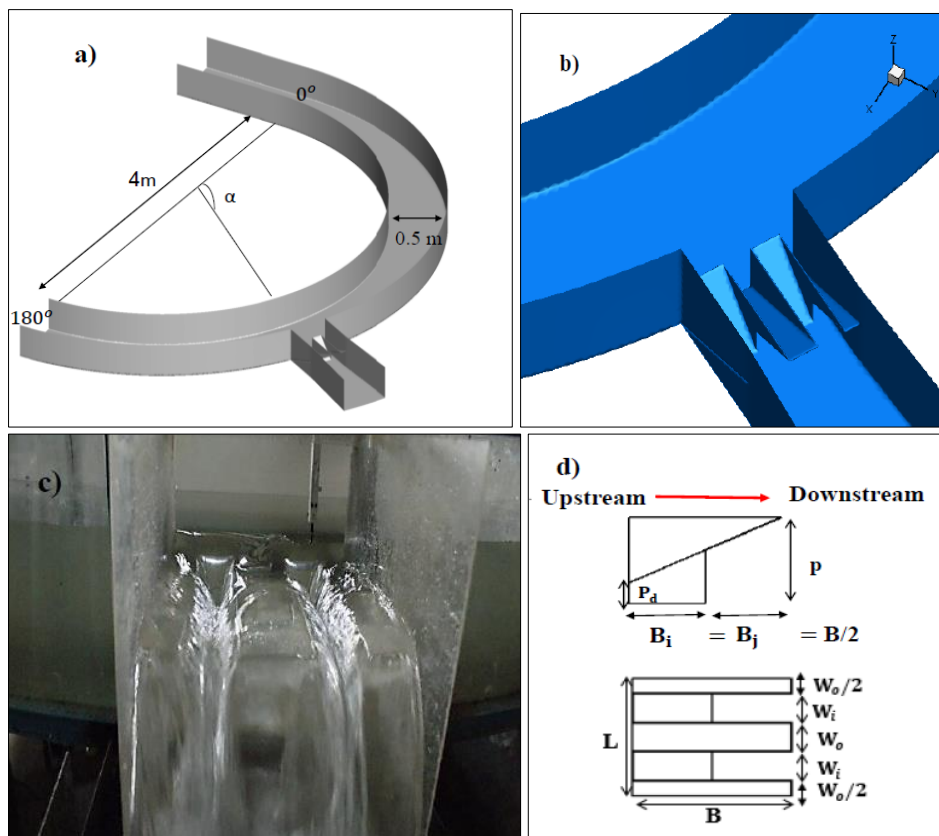

Figure 2. Schematic of the experimental setup, a) Plan of canal curve, b) Schematic of the PKSW, c) Schematic of

the PKSW in the experimental setup, d) Plan of PKSW

Table 2. The range of the variables used in the channel

Variable	Range
width of channel(m)	0.5
main channel depth (m)	0.5
channel slope	0.001
total discharge(l/s)	6.2-41
Froude number	0.042-0.31
length (width) of side weir (m)	0.15-0.25-0.35
radius of main channel centreline (m)	2.25

Table 3. The models of the C-type PKSW in the research

Types of models in simulation	P_d (cm)	L (cm)	$W_i=W_o$ (cm)	P (cm)	l (cm)	B (cm)
1 to 12	0.0, 3, 7, 10	15, 25, 35	3 to 8	6 to 24	75 to 175	15, 25, 35

3. Results and Discussion

3.1. Examination and Analysis of the Results Obtained from the C-type PKSW at the 120° Angle of the Curve

After installing the C-type PKSW at the 120° angle of the channel curve and conducting several tests using different Froude numbers and various proportions of the dimensionless parameters of L/b and $P/h1$, discharge changes were studied in the side weirs of the PKSW. The results are as follows:

3.1.1. Study of the Changes in the PKW Discharge Coefficient using Varied ratios of Fr, $\frac{L}{b}$ and $\frac{P}{h1}$

This research tests the discharge changes in the PKSW using varied Froude numbers. The water depth in the upstream was controlled by changing the downstream slide gate. Figure 3 shows the discharge coefficient of the PKSW in the weir with two dimensionless ratios of L/b=0.7 in proportion to the dimensionless parameter of $P/h1$ within the range of 0.5–0.9 at an angle of 120°.
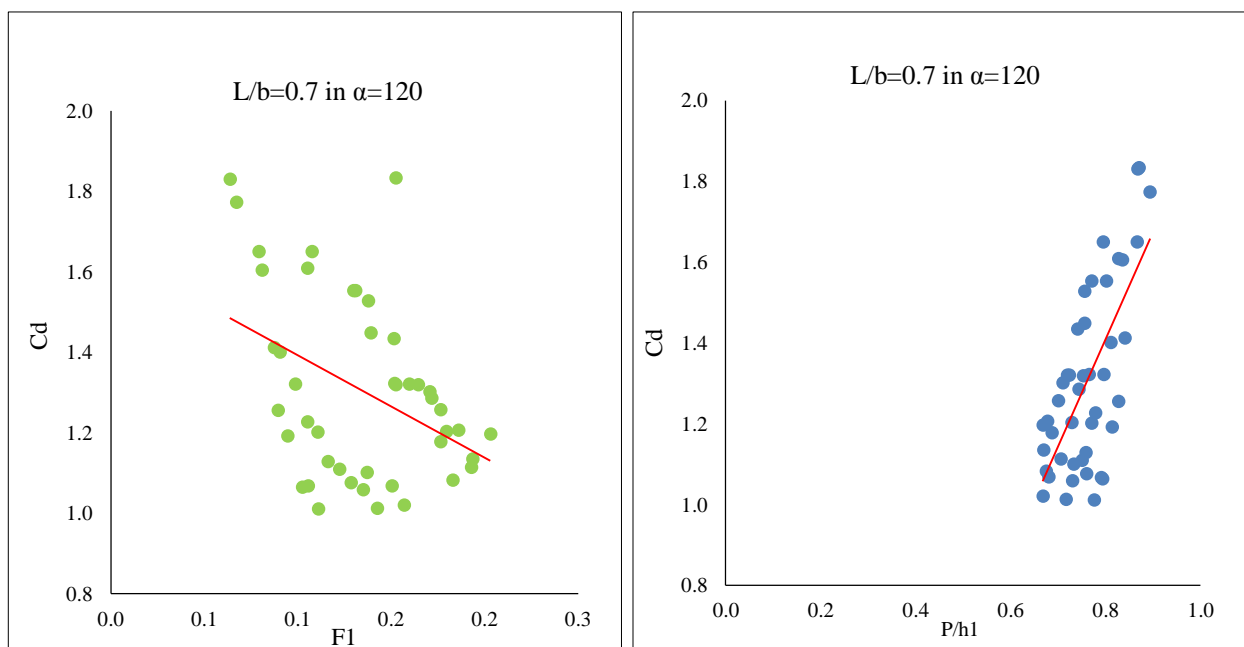

Figure 3. The effect of p/h₁ and Fr parameters on the discharge coefficient at an angle of 120°

It also shows the effect of Froude number on the discharge coefficient of the weir with the mentioned specifications within the Froude number range of 0.05–0.25 for the PKW. Figure 4 shows the changes in the discharge coefficient under the influence of $P/h1$ and F_1 on the discharge coefficient of the weir with the specifications of $L/b = 0.5$.
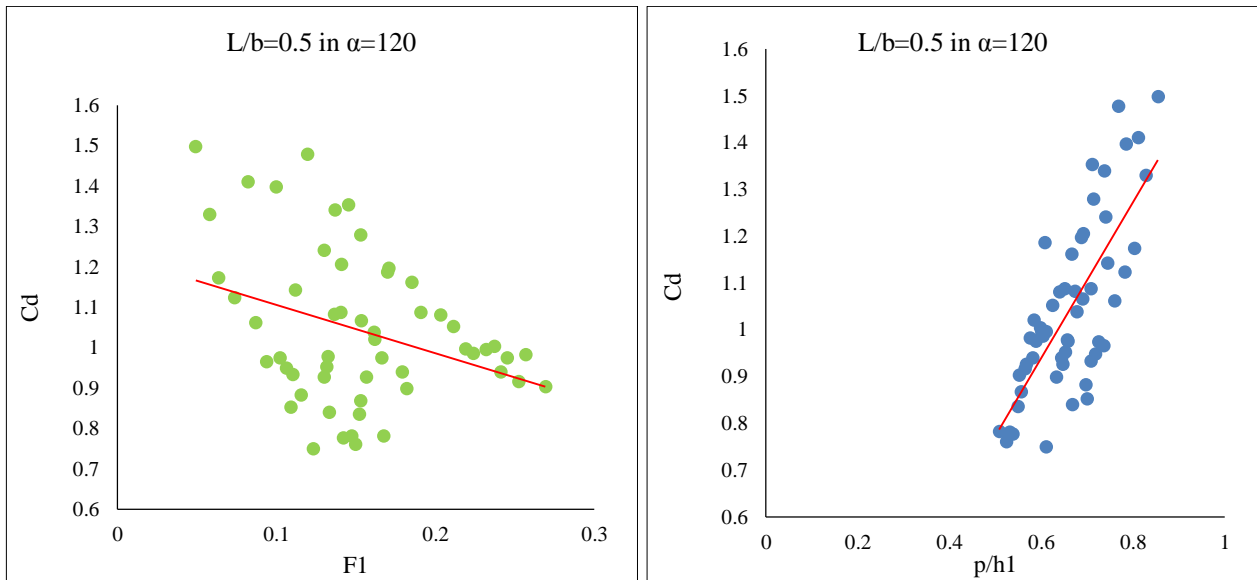
Figure 4. The effect of p/h₁ and F_r parameters on the discharge coefficient at an angle of 120°

Figure 5 shows the changes in the discharge coefficient that were affected by the effective parameters of $P/h1$ and Fr respectively in $L/b = 0.3$ and within the ranges of 0.2–0.8 and 0.05–0.25. The determination of the discharge coefficient of the PKSW at an angle of 120° of the curve shows that the discharge coefficient increases with the reduction of the length of the flow deviation and the increase of the secondary flow in the weir inlet. With respect to the submergence of PKSW edges and increases in the flow length, $P/h1$ reduces with the reduction in the discharge coefficient.
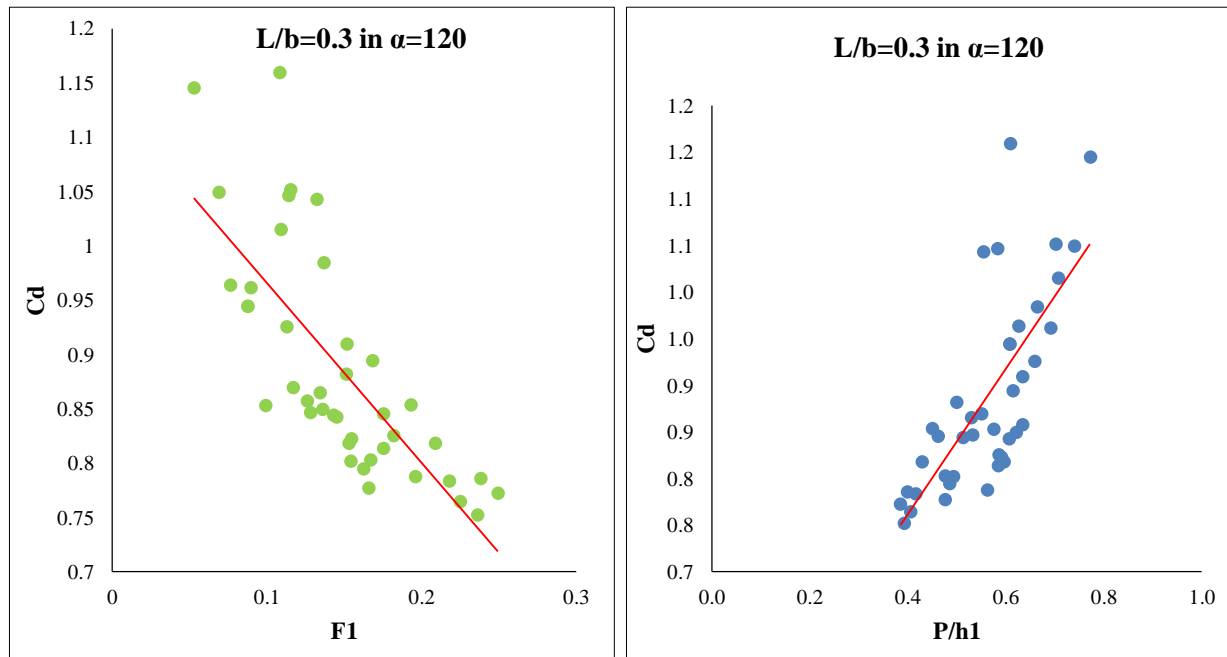

Figure 5. The effect of p/h₁ and F_r parameters on the discharge coefficient at an angle of 120°

3.2. Examination and Analysis of the Results Obtained from C-type PKSW at the 30° Angle of the Channel Curve

After installing the C-type PKSW at the 30° angle of the channel curve and conducting several tests using different Froude numbers and various proportions of the dimensionless parameters of $L/(b\ )$ and $P/h1$, the changes in the discharges were studied in the side weirs of the PKSW. The results are as follows:

3. 2.1. Study of the Changes in the PKSW Discharge Coefficient using Varied Proportions of Fr, $\frac{L}{b}$ and $\frac{P}{h1}$

Figure 6 shows the effect of the dimensionless ratio of Froude and $P/(h1\ )$on the discharge coefficient of the weir with L/b=0.7 specifications in the curved channels at an angle of 30°. The figure shows a direct relationship between parameter $P/h1$ and the weir discharge coefficient this can be attributed to the effect of submergence on the PKSW discharge coefficient. With the $P/h1$ increasing, all weir keys have an effective role in flow rate discharge and the flow passes freely through all the keys. However, the discharge coefficient reduces with decreases in $P/h1$, that is, with

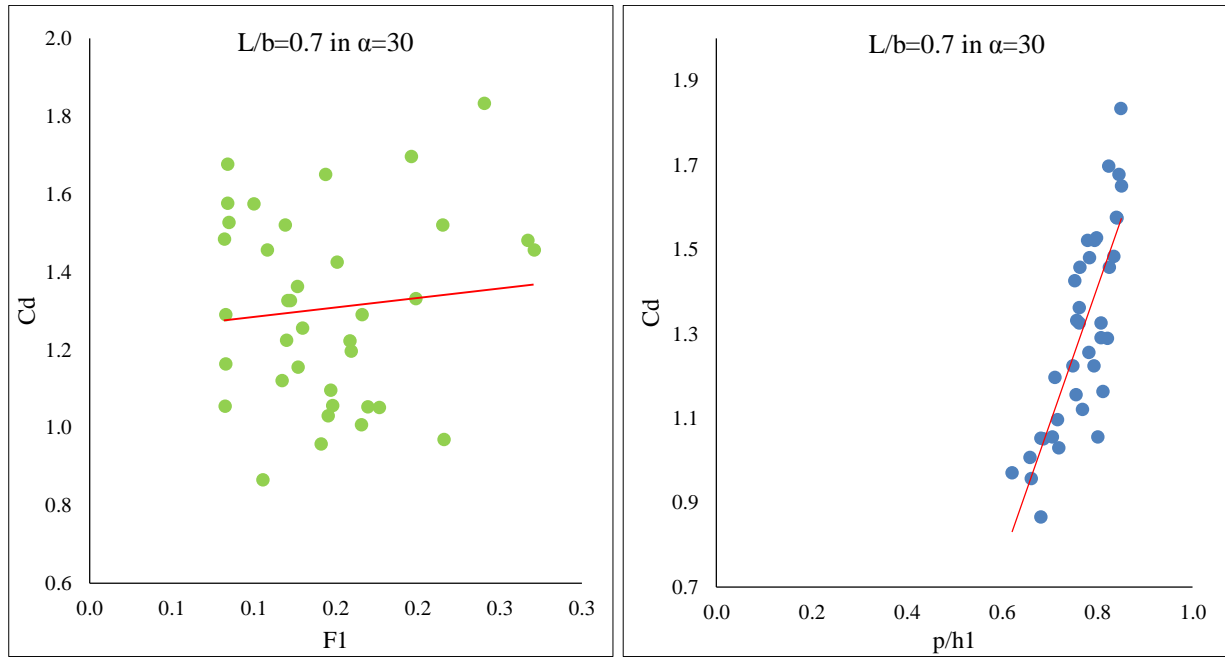increases in the flow depth in the channel.

Figure 6. The effect of p/h$_1$ and F$_r$ parameters on the discharge coefficient at an angle of 30°

This is owing to the secondary flows, the increases in the flow deviation length, and the increases in submergence in outlet keys and weir edges. This reduces the weir performance and leads to a lack of proper discharge of the weir. Figure 7 shows the effect of $P/h1$ and F_1 on the weir discharge coefficient with $L/b = 0.5$ specifications.
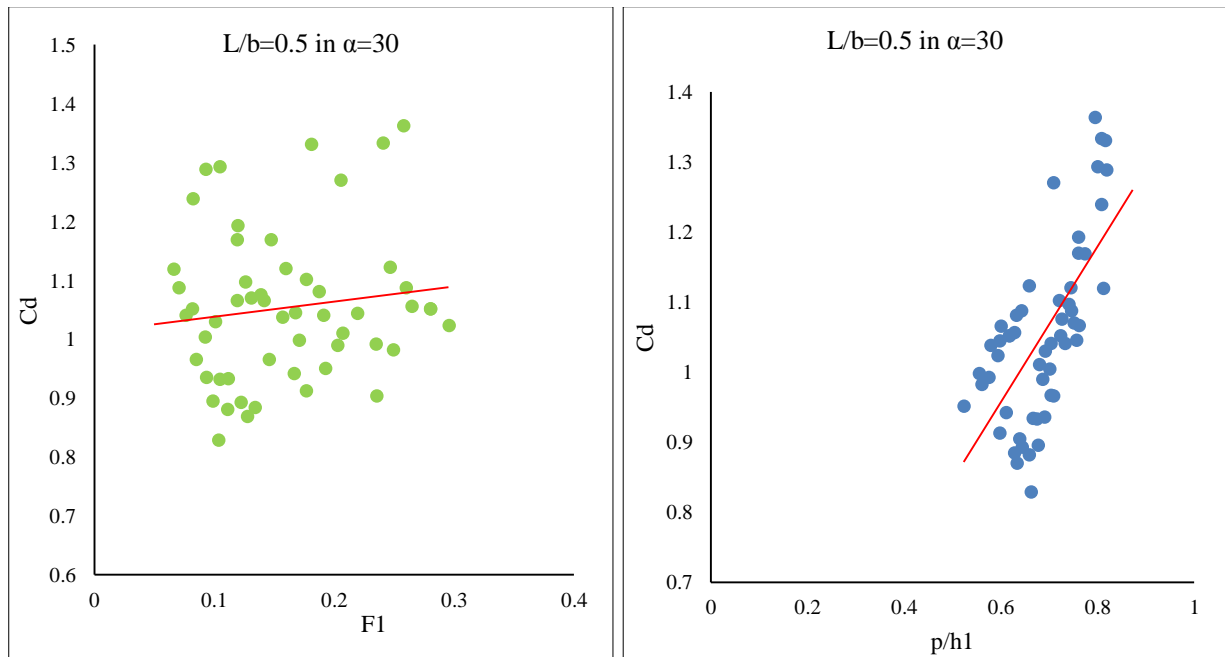

Figure 7. The effect of p/h$_1$ and F$_r$ parameters on the discharge coefficient at an angle of 30°

The figure shows that weir discharge increases with the $P/h1$ figure increasing and vice versa. It also shows that the Froude number has no considerable impact on the discharge coefficient of the weir at an angle of 30° of the curve. Figure 8 shows the effect of the dimensionless parameters of $P/h1$ and F1 on the weir discharge coefficient with L/b =0.3 specifications. The weir shows that the discharge coefficient increases with increase in the $P/h1$ and vice versa.
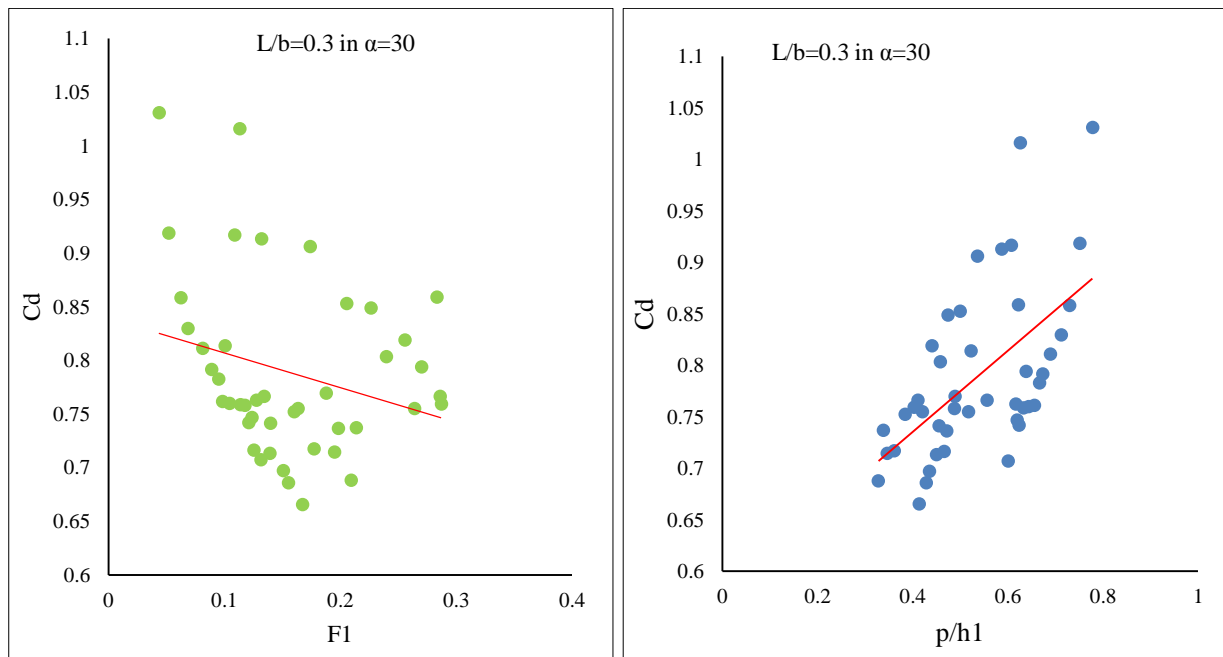
Figure 8. The effect of p/h₁ and Fᵣ parameters on the discharge coefficient at an angle of 30°

3. 3. Comparison of C-Type Piano Key Side Weirs at 30° and 120° Sections of a Curved Channel

In order to further analysis the output results of both Sections, as shown in Figure 9 the effect of the dimensionless ratio of $P/(h1)$ on the discharge coefficient of the C-Type Piano Key Side Weirs. Also, Figure 10 shows the effect of the dimensionless ratio of Froude on the discharge coefficient of the PKSW. The figure shows a direct relationship between parameter $P/h1$ and Cd.
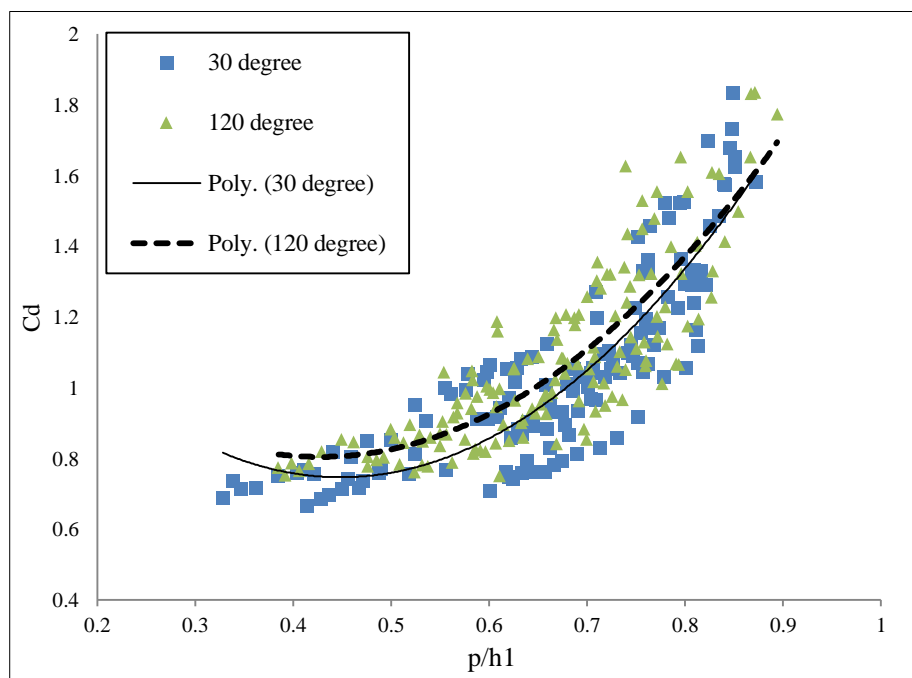

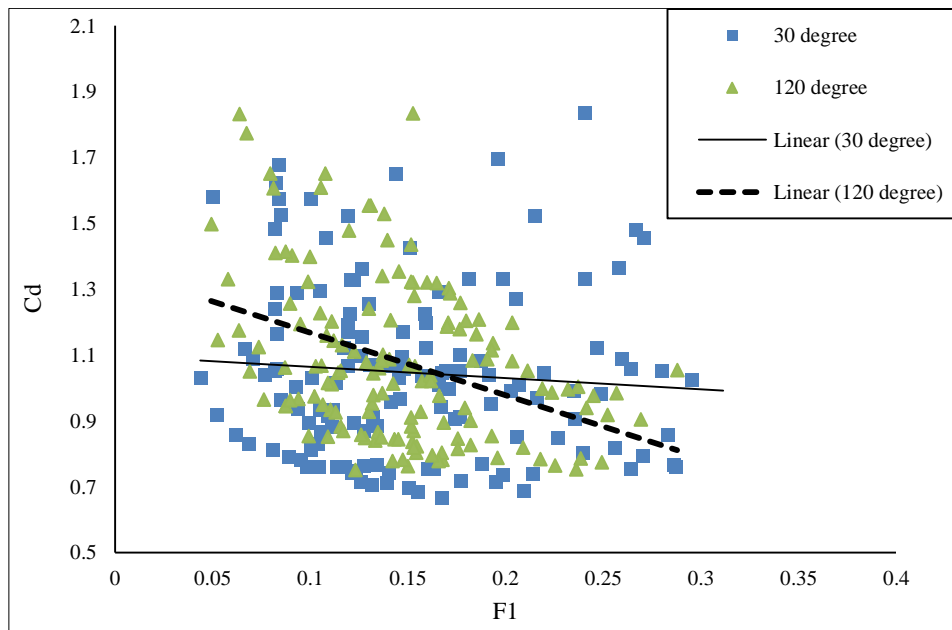**Figure 9. Comparison of the effect of p/h1 on Cd for C-Type Piano Key Side Weirs at 30° and 120° Section**

Figure 10. Comparison of the effect of Fr on Cd for C-Type Piano Key Side Weirs at 30° and 120° Sections

3.4. Presentation of a Discharge Coefficient Empirical Equation for the PKSW Side Weir

This research discusses an empirical relation to predict the discharge coefficient of a PKSW and to study its accuracy. A discharge coefficient was presented at the sections of 30° and 120° of the C-type weir using an empirical relationship between the effective inlet parameters and the outlet parameters in Equation 12. Equation 12 shows a proposed equation for the C-type PKSW side weir. It shows that the effect of the parameter $\frac{P}{h_1}$ on the discharge coefficient is greater than those of other parameters. Therefore, this is the most important parameter to design the weir under these conditions. It can be concluded from studying other parameters that the discharge coefficient never changes considerably by altering the parameters.

$$C_d = \exp(-0.06\frac{L}{b} - 0.153F_1 + 0.05\frac{L}{r_c} + 2.17\frac{p}{h_1} - 0.67\frac{p_d}{B} + 0.0001\alpha - 1.16) \tag{12}$$

Figure 11 compares the observational discharge coefficient and the computational discharge coefficient. The 45° line shows 100 percent accuracy. The figure and data distribution show that the presented relation has an acceptable accuracy with the correlation coefficient of 0.88 and an absolute error of 0.091. Consequently, the equation can be used for designing the PKSW side weir in the curve.
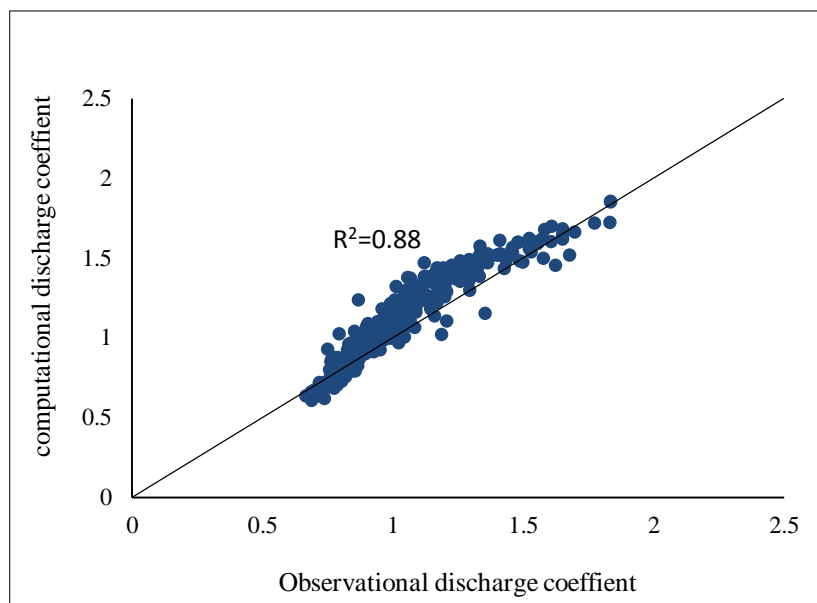

Figure 11. Studying the accuracy of the relation proposed for the PKSW

4. Conclusion

This research experimentally discusses the discharge coefficient of a PKSW side weir at 30° and 120° sections of a curved channel. To do so, different models of the weir were designed and accordingly prepared. The parameter P/h1 in PKSW affects the amount of the discharge coefficient at both 30° and 120° angles; it increases with increases in the value of the discharge coefficient. The effect of the parameter P/h1 on low values submerges the weir and reduces its performance. However, the effect of the parameter Fr at 30° is lower than its effect at 120°. Based on the dimensional analysis, an empirical equation was presented in Equation 12 for the discharge coefficient of the C-type side weir in two angles of the curve; the equation can be used for estimating the discharge coefficient of the PKSW. Furthermore, laboratory data analysis showed that the Froude number has no considerable impact on the discharge coefficient of the weir at the 30° angle of the curve. Also, the discharge coefficient decreased with increases in the Froude number of the weir at the 120° angle of the curve.

5. Acknowledgements

6. References

[1] Mahmodinia, S., M. Javan, and Afshin Eghbalzadeh. "The flow field and free surface pattern of the submerged side weir with different lengths." Arabian Journal for Science and Engineering 39.6 (April 2014): 4461-4472. doi: 10.1007/s13369-014-1058-y.

[2] Emin Emiroglu, M., M. Cihan Aydin, and Nihat Kaya. "Discharge characteristics of a trapezoidal labyrinth side weir with one and two cycles in subcritical flow." Journal of Irrigation and Drainage Engineering 140.5 (February 2014): 04014007. doi: 10.1061/(ASCE)IR.1943-4774.0000709.

[3] Lemperiere, F, and Ahmed Ouamane. "The Piano Keys weir: a new cost-effective solution for spillways." International Journal on Hydropower & Dams 10.5 (2003): 144-149.

[4] Kabiri-Samani, A, and Amir Javaheri. "Discharge coefficients for free and submerged flow over Piano Key weirs." Journal of Hydraulic Research 50.1 (August 2012): 114-120. doi: 10.1080/00221686.2011.647888.

[5] Agaccioglu, Hayrullah., M. Emin Emiroglu, and Nihat Kaya. "Discharge coefficient of side weirs in curved channels." Proceedings of the Institution of Civil Engineers-Water Management. Vol. 165. No. 6. Thomas Telford Ltd, (August 2012). doi: 10.1680/wama.11.00007.

[6] Agaccioglu, H, and Yalcin Yuksel. "Side-weir flow in curved channels." Journal of irrigation and drainage engineering 124.3 (May 1998): 163-175. doi:10.1061/(ASCE)0733-9437(1998)124:3(163).

[7] Cosar, A, and Hayrullah Agaccioglu. "Discharge coefficient of a triangular side-weir located on a curved channel." Journal of irrigation and drainage engineering 130.5 (October 2004): 410-423. doi: 10.1061/(ASCE)0733-9437(2004)130:5(410).

[8] Agaccioglu, H., F. Onen, and Fuat Toprak. "Scour around a side-weir at a 30 DG section of a 180 DG alluvial curved channel." Irrigation and Drainage 56.4 (June 2007): 423-438. doi: 10.1002/ird.304.

[9] Kaya, N., M. Emin Emiroglu, and Hayrullah Agaccioglu. "Discharge coefficient of a semi-elliptical side weir in subcritical flow." Flow Measurement and Instrumentation 22.1 (March 2011): 25-32. doi:10.1016/j.flowmeasinst.2010.11.002.

[10] Emiroglu, M, and Nihat Kaya. "Discharge coefficient for trapezoidal labyrinth side weir in subcritical flow." Water resources management 25.3 (December 2011): 1037-1058. doi: 10.1007/s11269-010-9740-7.

[11] Vatankhah, Ali R. "Analytical solution for water surface profile along a side weir in a triangular channel." Flow Measurement and Instrumentation 23.1 (March 2012): 76-79. doi: 10.1016/j.flowmeasinst.2011.10.001.

[12] Vatankhah, Ali R. "Water surface profile along a side weir in a parabolic channel." Flow Measurement and Instrumentation 32 (August 2013): 90-95. doi: 10.1016/j.flowmeasinst.2013.04.010.

[13] Azimi, H, and Saeid Shabanlou. "The flow pattern in triangular channels along the side weir for subcritical flow regime." Flow Measurement and Instrumentation 46 (December 2015): 170-178. doi: 10.1016/j.flowmeasinst.2015.04.003

[14] Aydin, M. Cihan, and Muhammet Emin Emiroglu. "Numerical analysis of subcritical flow over two-cycle trapezoidal labyrinth side weir." Flow Measurement and Instrumentation 48 (April 2016): 20-28. doi: 10.1016/j.flowmeasinst.2016.01.007.

[15] Tiwari, H, and Nayan Sharma. "Turbulent kinetic energy in the upstream of Piano Key Weir." Arabian Journal for Science and Engineering 41.10 (March 2016): 4147-4152. doi: 10.1007/s13369-016-2118-2.

[16] Ghasemzadeh, F., B, Parsa, and Mojtaba Noury. "Numerical study of overflow capacity of spillways (with an emphasis on PK-weirs)." E-proceedings of the 36th IAHR World Congress, Hague, The Netherlands. 2015.

[17] Hu, H., Z, Qian., W, Yang., D, Hou, and Dongmei Hou. "Numerical Study of Characteristics and Discharge Capacity of Piano Key Weirs." Flow Measurement and Instrumentation (August 2018). doi: 10.1016/j.flowmeasinst.2018.05.004.

[18] Al-Shukur, A, K., and Ghufraan H. Al-Khafaji. "Experimental study of the hydraulic performance of piano key weir."

International Journal of Energy & Environment 9.1 (2018).

[19] Mehboudi, A., J. Attari, and seyyedamirhossein Hosseini. "Experimental study of discharge coefficient for trapezoidal piano key weirs." Flow Measurement and Instrumentation 50 (August 2016): 65-72. doi:10.1016/j.flowmeasinst.2016.06.005.

[20] De Marchi, G. "Essay on the performance of lateral weirs." L'Energia Elettrica, Milan, Italy 11 (1934): 849-860.

[21] Borghei, S. M., M. R. Jalili, and Masoud Ghodsian. "Discharge coefficient for sharp-crested side weir in subcritical flow." Journal of Hydraulic Engineering 125.10 (October 1999): 1051-1056. doi: 10.1061/ (ASCE) 0733-9429(1999)125:10(1051).

[22] Subramanya, K, and Subhash Chandra Awasthy. "Spatially varied flow over side-weirs." Journal of the Hydraulics Division 98.1 (1972): 1-10.

[23] Nandesamoorthy, T., and A. Thomson. "Discussion of spatially varied flow over side weir." ASCE Journal of the Hydraulics Division 98.12 (1972): 2234-2235.

[24] Hager, W. H. "Lateral outflow over side weirs." Journal of Hydraulic Engineering 113.4 (April 1987): 491-504. doi: 10.1061/(ASCE)0733-9429 (1987)113:4(491).

[25] Ranga Raju, K., S. K. Gupta, and Baidyanath Prasad. "Side weir in rectangular channel." Journal of the Hydraulics Division 105.5 (1979): 547-554.

[26] Singh, R., D. Manivannan, and Tsnarayana Satyanarayana. "Discharge coefficient of rectangular side weirs." Journal of irrigation and drainage engineering 120.4 (July 1994): 814-819. doi:10.1061/(ASCE)0733-9437(1994)120:4(814).